

# Systematic Improvement of Molecular Excited State Calculations by Inclusion of Nuclear Quantum Motion

Timothy J. H. Hele<sup>1</sup>, Bartomeu Monserrat<sup>2,3</sup>, Antonios M. Alvertis<sup>3,\*</sup>

<sup>1</sup>Department of Chemistry, University College London, 20, Gordon Street, London WC1H 0AJ, United Kingdom

<sup>2</sup>Department of Materials Science and Metallurgy, University of Cambridge, 27 Charles Babbage Road, Cambridge CB3 0FS,  
United Kingdom

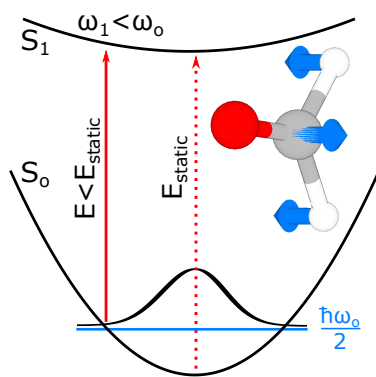
<sup>3</sup>Cavendish Laboratory, University of Cambridge, J. J. Thomson Avenue, Cambridge CB3 0HE, United Kingdom

\*e-mail: ama80@cam.ac.uk

## Abstract

Many theoretical studies of molecular excited states aim to provide accurate solutions to the electronic Schrödinger equation in order to produce energies that can be compared to experiment. However, the role of nuclear quantum effects is usually overlooked. Here we provide an intuitive picture for this effect and find that nuclear quantum fluctuations almost always lower the energies of excited states from the conventional vertical excitation energy. We compute the vibration-induced corrections to the exciton energies of the commonly used Thiel set of molecules by combining TD-DFT with Monte Carlo sampling techniques based on finite difference methods, and find corrections as large as 1.1 eV. We compare our results for the exciton energies to uncorrected TD-DFT and the accurate reference Thiel values, finding that incorporating nuclear quantum motion substantially improves agreement with experiment, at a low computational cost. Accounting for nuclear quantum motion is therefore established as a critical factor towards the accurate calculation of exciton energies in molecules.

# TOC graphic



The optoelectronic properties of organic molecules are dominated by their low-lying excited states known as excitons [1]. Exciton energies are critical to several technologically-relevant processes in these systems, such as singlet fission and thermally activated delayed fluorescence, which find applications in photovoltaics and LEDs respectively [2, 3]. It is therefore desirable to develop methods for the accurate prediction of exciton energies.

Typical methods for the calculation of excited state energies, such as time-dependent density functional theory (TD-DFT) [4], complete active space self-consistent field (CAS-SCF) [5] and the Bethe-Salpeter equation (BSE) [6, 7, 8], only account for electronic effects on exciton states, typically computing these at a fixed geometry of the studied system. However, even at 0 K, atomic nuclei vibrate according to normal modes with a zero-point energy of  $\frac{1}{2}\hbar\omega$ . In a recent study on solid state organic semiconductors [9], two of us showed that nuclear quantum motion can significantly change exciton energies computed at the ground state geometry of a system, and that incorporating these effects leads to improved agreement with experiment.

Here we systematically investigate the effect of nuclear quantum motion on the exciton energies of organic molecules. We provide an intuitive explanation of why this will lead to a red shift of exciton energies in the vast majority of molecules, and based on a harmonic approximation we derive an analytic expression quantifying this effect and relating it to the frequency difference between the vibrational normal modes of the ground and excited states. Although this simple model provides useful insights, quantitative calculations often require a more sophisticated treatment due to the anharmonic character of excited state potential energy surfaces.

We therefore use a Monte Carlo sampling technique, combining TD-DFT and finite difference methods for the molecular vibrations [10, 11], allowing us to treat excited state energy surfaces without any harmonic assumption. We apply this method to the so-called Thiel set of organic molecules, for which highly accurate exciton energies have been computed using wavefunction-based methods [12]. The Thiel set of molecules consists of four broad categories of structures: unsaturated aliphatic hydrocarbons, aromatic hydrocarbons and heterocycles, carbonyl compounds, and nucleobases. A full list of the studied structures is given in section S1 of the Supporting Information (SI). It has become common in the literature to compare new methods for the calculation of exciton energies to the Thiel set [13, 7, 14, 15, 8], a path that we also take. Remarkably, we find that the inclusion of nuclear quantum effects into our TD-DFT calculations leads to significantly better agreement with experimental results than both the (uncorrected) TD-DFT and high-level Thiel calculations. This highlights the fact that corrections to exciton energies due to nuclear quantum motion can be as important, and occasionally more important than those that are calculated via highly accurate beyond-TD-DFT electronic structure calculations; an effect that is even more pronounced for small molecules with very strong exciton-vibration interactions. The method we use is computationally inexpensive compared to the highly accurate electronic structure methods used to go beyond TD-DFT, making it a practical way of achieving greater accuracy in exciton energy calculations. While here we employ TD-DFT to solve the electronic structure problem, our methodology for correcting exciton energies can be used in conjunction with any electronic structure method, including high-level techniques such as CAS-SCF.

Let us start with a qualitative discussion of the effects of nuclear quantum motion on exciton energies. In organic molecules, the highest occupied molecular orbital (HOMO) is a bonding  $\pi$  orbital that lowers the energy

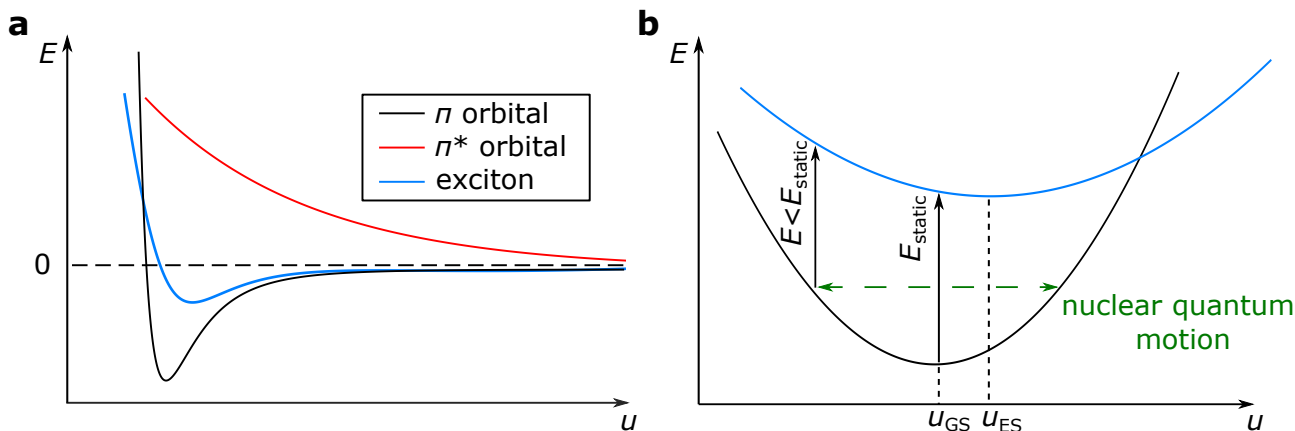


**Figure 1** Schematic representation of the energy of a  $\pi$  and  $\pi^*$  orbital, as well as the exciton state that results from a transition between them, along a generalized coordinate  $u$  (panel **a**). Due to the excited state potential energy surface being less steep, nuclear quantum motion leads to a red-shift of the energy difference between the ground and excited states compared to its static value (panel **b**).

of the molecule once occupied and leads to nuclei that are closer to each other. Therefore, the energy of such a  $\pi$  orbital along a generalized nuclear coordinate  $u$  of the molecular system will look similar to a Morse potential, as visualized in Figure 1a (black). The lowest unoccupied molecular orbital (LUMO) is an anti-bonding  $\pi^*$  orbital that raises the energy of the molecule once occupied and forces the nuclei apart, its energy along  $u$  showing an exponential decay (Figure 1a, red). For most conjugated organic molecules, the lowest energy singlet exciton ( $S_1$ ) is formed by exciting an electron from the HOMO to the LUMO [16], with energy:

$$E(S_1) = E(S_0) + \epsilon_L - \epsilon_H - J_{HL} + 2K_{HL}. \quad (1)$$

Here  $E(S_0)$  is the energy of the ground state,  $\epsilon_H$  and  $\epsilon_L$  are the energies of the HOMO and the LUMO respectively,  $J_{HL}$  the HOMO-LUMO Coulomb integral and  $K_{HL}$  the HOMO-LUMO exchange integral. By using equation 1, we schematically describe the energy of an exciton along  $u$  (Figure 1a, blue), having assumed that the dependence of the integrals  $J, K$  on  $u$  does not alter its qualitative characteristics.

What can be observed from Figure 1a is that the excited state potential energy curve (blue) is less steep compared to the ground state one (black). Therefore, if we approximate the two within the harmonic approximation, we obtain two parabolas of different curvature, as shown in Figure 1b. If the structure was ‘frozen’ at its ground state configuration  $u_{GS}$ , then the energy required to access the exciton state would be  $E_{static}$ , which is the energy gap usually computed by electronic structure calculations. However, due to the quantum motion of the nuclei, the system can explore a distribution of configurations within the region denoted by green arrows, even at 0 K. If we excited the system from any given displaced configuration within the available region, then the excitation energy becomes smaller than  $E_{static}$ , since the lower parabola corresponding to the ground state is steeper (has higher frequency) than the excited state one. Therefore, it is expected that inclusion of the effects of nuclear quantum fluctuations will lead to a red-shift of exciton energies. Naturally, thermal motion of the nuclei will have a similar result on exciton energies, however the light mass of the constituent elements

of organic molecules leads to vibrational modes with high frequencies, which are only weakly activated at room temperature. Additionally, thermal nuclear motion mostly affects the energies of the spatially extended excited states that crystalline systems can host [9], which is not the scenario we are examining here. We therefore focus on nuclear motion at  $T = 0$  K, however our presented method could be used to study exciton-vibration interactions at any temperature.

Now let us quantify the change in exciton energies due to nuclear quantum motion. At temperature  $T$ , we include the contribution of molecular vibrations to the exciton energy  $E_{\text{exc}}(T)$  by means of the standard quantum mechanical expectation value:

$$E_{\text{exc}}(T) = \frac{1}{\mathcal{Z}} \sum_{\mathbf{s}} \langle \chi_{\mathbf{s}}(\mathbf{u}) | E_{\text{exc}}(\mathbf{u}) | \chi_{\mathbf{s}}(\mathbf{u}) \rangle e^{-E_{\mathbf{s}}/k_{\text{B}}T}, \quad (2)$$

where  $|\chi_{\mathbf{s}}(\mathbf{u})\rangle$  is a vibrational eigenstate on the ground state potential energy surface with energy  $E_{\mathbf{s}}$ ,  $\mathcal{Z} = \sum_{\mathbf{s}} e^{-E_{\mathbf{s}}/k_{\text{B}}T}$  is the partition function, and  $\mathbf{u}$  is the nuclear displacement. To simplify the problem, we resort to the harmonic approximation for the ground state potential, and by substituting  $|\chi_{\mathbf{s}}(\mathbf{u})\rangle$  with the wavefunction of a quantum harmonic oscillator we obtain [11]:

$$E_{\text{exc}}(T) = \int d\mathbf{u} |\Phi(\mathbf{u}; T)|^2 E_{\text{exc}}(\mathbf{u}), \quad (3)$$

where:

$$|\Phi(\mathbf{u}; T)|^2 = \prod_{\nu} (2\pi\sigma_{\nu}^2(T))^{-1/2} \exp\left\{\left(-\frac{u_{\nu}^2}{2\sigma_{\nu}^2(T)}\right)\right\}, \quad (4)$$

is the harmonic density at temperature  $T$ , which in turn is a product of Gaussian functions of width:

$$\sigma_{\nu}^2(T) = \frac{1}{2\omega_{\nu}} \cdot \coth\left(\frac{\omega_{\nu}}{2k_{\text{B}}T}\right). \quad (5)$$

In the above, atomic units and mass-weighted coordinates have been used, and  $\nu$  is the index labeling the ground state vibrational modes of the studied molecule. In order to make further progress, we assume that the excited state surface is also parabolic, and taking the limit of  $T = 0$  K we find:

$$E(T = 0 \text{ K}) = E_{\text{static}} - \frac{1}{4} \sum_{i=1}^{3N-6} \frac{\omega_{G_i}^2 - \omega_{E_i}^2}{\omega_{G_i}} \quad (6)$$

where  $\omega_{G_i}$  and  $\omega_{E_i}$  are the frequencies of the vibrational mode  $i$  of the ground and excited state respectively. For a molecule with  $N$  atoms, there are  $3N - 6$  non-trivial vibrational modes in total, and equation 6 suggests that as expected  $E(T = 0 \text{ K}) < E_{\text{static}}$ , given that the potential energy surface of the ground state is steeper than that of the excited state and therefore  $\omega_{G_i}^2 > \omega_{E_i}^2$ . The full derivation of equation 6 is provided in section S4 of the SI.

While equation 6 confirms the intuitive expectation that nuclear quantum motion leads to a red shift of exciton energies, the assumption that the excited state surface along vibrational normal modes is harmonic is

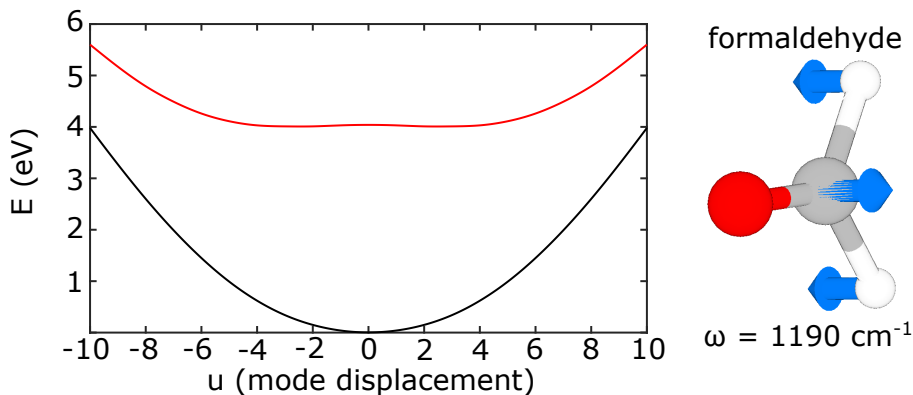


**Figure 2** Ground (black) and excited state (red) potential energy surfaces of formaldehyde (left) along a vibrational mode with frequency  $1190\text{ cm}^{-1}$ .

often violated. Examples of strongly anharmonic excited state potentials are known from the literature [17, 18], and here we exemplify this with the simulated potential energy surfaces of formaldehyde, shown in Figure 2. Therefore, equation 6 is of mostly qualitative value and one needs to go beyond this model in order to achieve quantitative accuracy. However, we emphasize that treating the ground state potential energy surface along vibrational eigenstates as harmonic remains a good approximation in many situations.

To do so, we evaluate the integral in equation 3 using Monte Carlo techniques, generating 100 configurations at  $T = 0\text{ K}$  distributed according to the corresponding harmonic density. Then, the expectation value of equation 3 is computed as the simple average of the computed values of the exciton energy  $E_{\text{exc}}(\mathbf{u})$  at the displaced configurations. To compute the exciton energies, we employ TD-DFT using the popular B3LYP hybrid functional [19] and the cc-pVDZ basis set, as implemented within the NWChem code [20]. This computational approach relies on no adjustable parameters, apart from those in the DFT functional, which are fixed throughout the entire series of calculations. We hence obtain zero-point renormalized (ZPR) exciton energies compared to those of a ‘static’ TD-DFT calculation for the Thiel set of molecules. We generally find that approximately 50 points are sufficient to sample the expectation value of the exciton energies. The numerical results of these calculations are given in SI section S2, not only at the B3LYP level, but also for three additional DFT functionals as discussed below.

We now proceed to compare the energies of the singlet excitons obtained within our TD-DFT+ZPR approach that includes nuclear quantum motion to the experimental values collected in the original publication on the Thiel set [12]. We also compare the values obtained from ‘static’ TD-DFT and from highly accurate complete active space second-order perturbation theory (CASPT2) [21] calculations in the original Thiel publication [12] to experiment. The computed exciton energies always refer to single excitations as described within TD-DFT, and we exclude any double-excitations (bi-excitons) from our analysis, which are however accessible using wavefunction-based methods [12]. In Figure 3 we plot the computed versus experimental values for the three approaches, for all the studied molecules for which experimental data exists. The closer a point lies to the  $y = x$  line, the better the agreement between theory and experiment. We fit a linear model to the three sets of results, as a means of visualizing the overall agreement with experiment, from where it becomes evident that

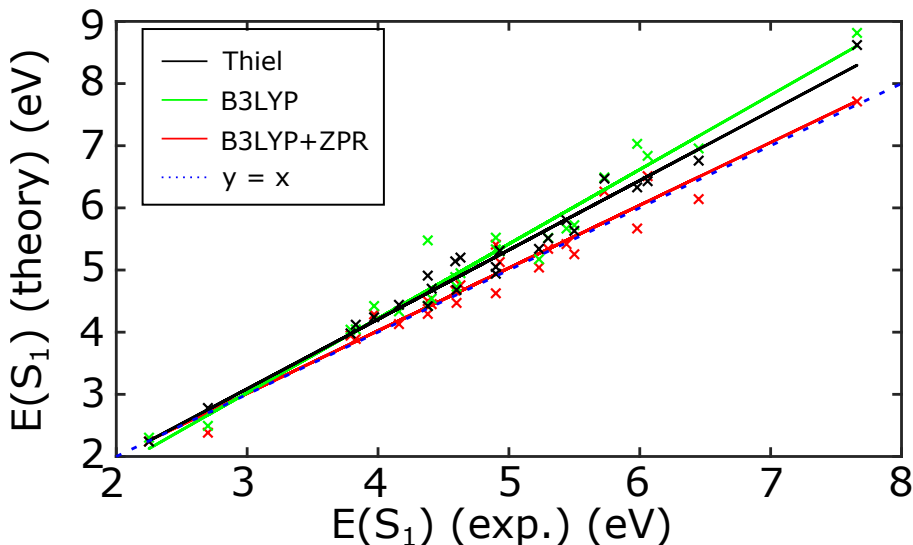


**Figure 3** Comparison of the different methods used to obtain the singlet exciton energies of the Thiel set to experiment. A ‘static’ TD-DFT approach at the B3LYP level (green) performs the worst, and accurate wavefunction-based methods reported in the literature (the values in black refer to the CASPT2 Thiel values [12] for single excitations, corresponding to the states computed within TD-DFT here). However, accounting for the zero-point renormalization (ZPR) of exciton energies due to molecular quantum fluctuations leads to the best agreement with experiment (red), even when ignoring beyond-TD-DFT electronic effects.

the TD-DFT B3LYP+ZPR (red) results provide a significant improvement to the static TD-DFT B3LYP values (green). The parameters for all the linear fits are given in SI section S3. Remarkably, we find that the values we compute with the inclusion of nuclear quantum fluctuations are in better agreement with experiment even compared to the benchmark Thiel values (black) that were obtained using accurate wavefunction-based methods. While naturally the Thiel values provide an improvement to static TD-DFT, the correction to exciton energies induced by the quantum fluctuations of molecular vibrations seems to be more significant than corrections due to beyond-TD-DFT electronic effects. We now proceed to further quantify these comparisons.

We employ four different statistical measures in order to compare the accuracy of the different methods presented in Figure 3, which we summarize in Table 1. In particular, for our  $n = 24$  studied molecules with computed exciton energies  $b_i$  and experimental exciton energies  $a_i$ , we compute the average values of the bias:  $\text{bias} = \frac{1}{n} \sum_i (b_i - a_i)$ , the root mean-squared error:  $\text{RMSE} = \sqrt{\frac{1}{n} \sum_i (b_i - a_i)^2}$ , as well as the relative values to these quantities:  $(\text{rel.bias}) = \frac{1}{n} \sum \frac{b_i - a_i}{a_i}$ ,  $(\text{rel.RMSE}) = \sqrt{\frac{1}{N} \sum_i \frac{(b_i - a_i)^2}{a_i^2}}$ . The reason that we also consider the relative quantities is that the largest errors for the static TD-DFT and Thiel approaches are found in the region of large exciton energies, hence these molecules dominate the bias and root mean-squared error. For example, the static TD-DFT exciton energy of ethene is renormalized from 8.8 eV to 7.7 eV once we account for nuclear quantum effects. Using the relative bias and root mean-squared error, which are calculated by dividing by  $a_i$  and  $a_i^2$  respectively, we achieve a fairer comparison without under-representing the effect of molecules with lower exciton energies. We see from Table 1 that the average value of all the employed statistical measures is minimized when using TD-DFT at the B3LYP level combined with the zero-point renormalization (B3LYP+ZPR) of exciton energies due to molecular vibrations. We therefore quantitatively confirm the observation of Figure 3: corrections to static exciton energies due to nuclear quantum motion are generally larger than corrections due

	bias (eV)	rel.bias	RMSE (eV)	rel.RMSE
B3LYP	0.385	0.073	0.523	0.098
Thiel	0.303	0.060	0.380	0.072
B3LYP+ZPR	0.031	0.005	0.245	0.051

**Table 1** Statistical measures of the accuracy of the different methods. The average values of the (relative) bias and the (relative) root mean-squared error (RMSE) as defined in the text are given.

to beyond-TD-DFT electronic effects that are included in the Thiel values. We also quantify the spread of the four statistical quantities around their average value by computing their standard deviation, which is given in SI Table S32. We find that the spread of the B3LYP+ZPR values is in every case comparable to that of the Thiel values, and significantly smaller than that of the static TD-DFT (B3LYP) values.

Ideally, one would combine accurate electronic structure calculations with our approach for accounting for nuclear quantum motion. However, for most of the studied molecules we found that a minimum of approximately 50 points is required to converge the Monte Carlo sampling of the integral in equation 3. While the cost of 50 TD-DFT calculations of small molecules is reasonably low, it quickly becomes very high as one moves to more accurate wavefunction-based methods. It is therefore reasonable to wonder whether the vibrational corrections to exciton energies could be computed at one (cheaper) level of theory and applied to the static exciton energy obtained at another (more accurate) level of theory. To check whether the vibrational correction to exciton energies changes when using different electronic structure methods, we repeated our Monte Carlo sampling within three additional levels of TD-DFT, while using the vibrational modes obtained at the B3LYP level. In particular, for the excited state calculations we used the local density approximation (LDA), the generalized gradient approximation (GGA) as well as a functional with pure Hartree-Fock exchange. The results are presented in SI section S3. We find that the correction to static exciton energies can change significantly depending on the employed functional, suggesting it is not possible to accurately obtain the static and displaced exciton values at different levels of theory. Additionally, we find for most molecules at the LDA level that computing both the vibrational modes and excited states using this functional leads to small changes to the corrections of exciton energies, compared to using B3LYP vibrations along with LDA excited state calculations. Therefore, the change in the exciton energy correction between the different functionals seems to be due to changes in the excited state wavefunction and not in the molecular vibrational properties.

We found in Ref. [9] for solid state systems that the correction to exciton energies due to nuclear quantum motion becomes more important for smaller molecules. For the single-molecule systems studied here we find that the same trend holds, as shown in Figure 4 for the acene and aliphatic hydrocarbons families of molecules. This is because smaller molecules have a greater electronic density in the vicinity of localized carbon motions that are activated due to quantum fluctuations, hence leading to stronger exciton-vibration interactions. Another way of reaching the same conclusion is using Hückel theory. Let us consider the example of linear polyenes, such as ethene, butadiene, hexatriene and octatetraene that are studied here and are included among other aliphatic hydrocarbons in Figure 4b, showing a decrease in the exciton energy correction with increasing system size. For a linear polyene consisting of  $N$  carbon atoms, Hückel theory predicts the energy of the  $i^{\text{th}}$  orbital is:



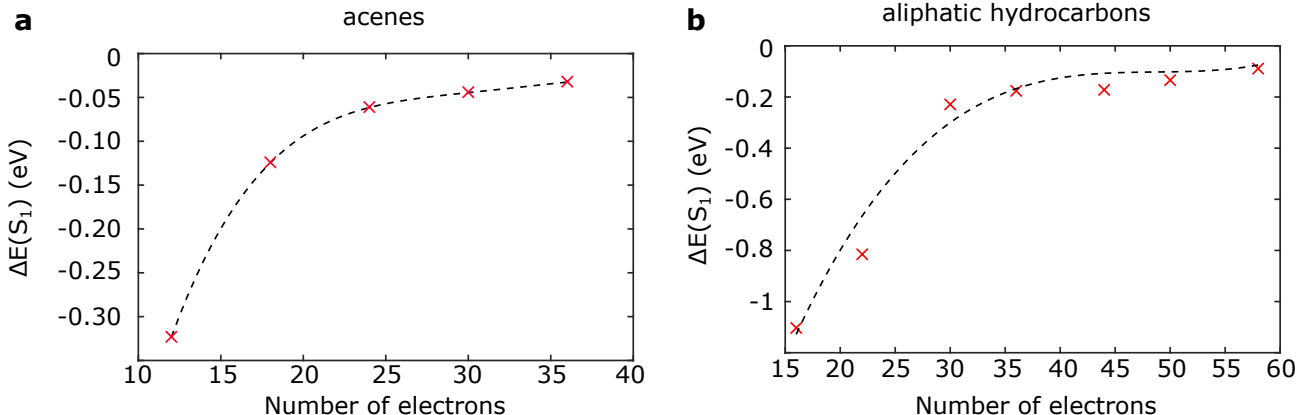


**Figure 4** Size dependence of the correction due to nuclear quantum motion to the singlet exciton energies  $\Delta E(S_1)$  of the acene (panel **a**) and aliphatic hydrocarbon (panel **b**) families of molecules.

$E_i = \alpha + 2\beta \cos(2\pi n/(N+1))$ , with  $\alpha, \beta$  the Hückel parameters, and  $i = 1, 2, \dots, N$ . From this, we find for the HOMO-LUMO gap:

$$E_{\text{gap}} \propto \sin\left(\frac{\pi}{2(N+1)}\right). \quad (7)$$

In the limit of  $N \rightarrow \infty$ , this gives  $E_{\text{gap}} \propto 1/N$ . A similar result can be obtained for cyclic polyenes. Assuming that the same holds for any general conjugated molecule, this suggests that in larger systems the HOMO is less bonding and the LUMO less anti-bonding than in comparably smaller systems. Therefore, from the intuitive picture of Figure 1, the curvature of the ground and excited state surfaces of large molecules is similar, and the difference in their normal mode frequencies is small. Hence, according to the qualitative expression 6, the correction to the exciton energy is also smaller than that for a smaller molecule. This is encouraging, in the sense that corrections due to nuclear quantum motion are mostly important for small systems, for which they are cheaper to compute.

In conclusion, we have presented an intuitive picture and a computational approach for estimating the effects of nuclear quantum motion on molecular exciton energies, which we show can indeed be substantial, particularly for smaller molecules. The corrections that molecular vibrations induce to exciton energies computed at a static level are found to be greater than corrections due to beyond-TD-DFT electronic effects as these were identified in previous studies. One could further improve upon these results by combining our computational methodology for nuclear quantum effects with a high-level theory of electronic structure, such as CAS-SCF. Overall, we underline the need for the community to explore nuclear quantum motion as a promising avenue for achieving quantitative accuracy when computing molecular excited state energies. While here we do not provide a mode-resolved picture, exploring which vibrational modes provide the largest correction to exciton energies could be of great interest and will be the subject of a future work.

## Data availability

The data underlying this publication can be found under [URL added in proof].

## Acknowledgments

The authors acknowledge useful discussions with Stuart Althorpe (Cambridge) and the support of the Winton Programme for the Physics of Sustainability. T.J.H.H. acknowledges a Royal Society University Research Fellowship Ref: URF\R1\201502. B.M. acknowledges support from the Gianna Angelopoulos Programme for Science, Technology, and Innovation. A.M.A. acknowledges the support of the Engineering and Physical Sciences Research Council for funding under grant EP/L015552/1.

## References

- [1] J. Frenkel. On the transformation of light into heat in solids. I. *Physical Review*, 37:17–44, 1931.
- [2] Akshay Rao and Richard H Friend. Harnessing singlet exciton fission to break the Shockley–Queisser limit. *Nature Reviews Materials*, 2:17063, October 2017.
- [3] Sebastian Reineke. Organic light-emitting diodes: Phosphorescence meets its match. *Nature Photonics*, 8(4):269–270, 2014.
- [4] M. Petersilka, U. J. Gossmann, and E. K.U. Gross. Excitation energies from time-dependent density-functional theory. *Physical Review Letters*, 76(8):1212–1215, 1996.
- [5] Per Åke Malmqvist and Björn O. Roos. The CASSCF state interaction method. *Chemical Physics Letters*, 155(2):189–194, 1989.
- [6] Michael Rohlfing and Steven G. Louie. Electron-hole excitations and optical spectra from first principles. *Physical Review B - Condensed Matter and Materials Physics*, 62(8):4927–4944, 2000.
- [7] Denis Jacquemin, Ivan Duchemin, and Xavier Blase. Benchmarking the Bethe-Salpeter Formalism on a Standard Organic Molecular Set. *Journal of Chemical Theory and Computation*, 11(7):3290–3304, 2015.
- [8] Denis Jacquemin, Ivan Duchemin, Aymeric Blondel, and Xavier Blase. Benchmark of Bethe-Salpeter for Triplet Excited-States. *Journal of Chemical Theory and Computation*, 13(2):767–783, 2017.
- [9] Antonios M. Alvertis, Raj Pandya, Loreta A. Muscarella, Nipun Sawhney, Malgorzata Nguyen, Bruno Ehrler, Akshay Rao, Richard H. Friend, Alex W. Chin, and Bartomeu Monserrat. Impact of exciton delocalization on exciton-vibration interactions in organic semiconductors. *Physical Review B - Condensed Matter and Materials Physics*, 102:081122(R), 2020.

- [10] K. Kunc and Richard M. Martin. Ab initio force constants of GaAs: A new approach to calculation of phonons and dielectric properties. *Physical Review Letters*, 48(6):406–409, 1982.
- [11] Bartomeu Monserrat. Electron – phonon coupling from finite differences. *Journal of Physics Condensed Matter*, 30, 2018.
- [12] Marko Schreiber, Mario R. Silva-Junior, Stephan P.A. Sauer, and Walter Thiel. Benchmarks for electronically excited states: CASPT2, CC2, CCSD, and CC3. *Journal of Chemical Physics*, 128(13), 2008.
- [13] Subhayan Roychoudhury, Stefano Sanvito, and David D. O’Regan. Neutral excitation density-functional theory: an efficient and variational first-principles method for simulating neutral excitations in molecules. *Scientific Reports*, 10(1):1–12, 2020.
- [14] Fabien Bruneval, Samia M. Hamed, and Jeffrey B. Neaton. A systematic benchmark of the ab initio Bethe-Salpeter equation approach for low-lying optical excitations of small organic molecules. *Journal of Chemical Physics*, 142(24), 2015.
- [15] Tonatiuh Rangel, Samia M. Hamed, Fabien Bruneval, and Jeffrey B. Neaton. An assessment of low-lying excitation energies and triplet instabilities of organic molecules with an ab initio Bethe-Salpeter equation approach and the Tamm-Dancoff approximation. *Journal of Chemical Physics*, 146(19), 2017.
- [16] P. W. (Peter William) Atkins. *Molecular quantum mechanics*. Oxford University Press, New York, 4th ed. / peter atkins, ronald friedman. edition, 2005.
- [17] Franco Egidi, David B. Williams-Young, Alberto Baiardi, Julien Bloino, Giovanni Scalmani, Michael J. Frisch, Xiaosong Li, and Vincenzo Barone. Effective Inclusion of Mechanical and Electrical Anharmonicity in Excited Electronic States: VPT2-TDDFT Route. *Journal of Chemical Theory and Computation*, 13(6):2789–2803, 2017.
- [18] Antonios M Alvertis, Steven Lukman, Timothy J H Hele, Eric G Fuemmeler, Jiaqi Feng, Jishan Wu, Neil C Greenham, Alex W Chin, and Andrew J Musser. Switching between Coherent and Incoherent Singlet Fission via Solvent-Induced Symmetry Breaking. *Journal of the American Chemical Society*, 141:17558–17570, 2019.
- [19] Axel D. Becke. A new mixing of Hartree-Fock and local density-functional theories. *The Journal of Chemical Physics*, 98(2):1372–1377, 1993.
- [20] E. Aprà *et al.* NWChem: Past, present, and future. *The Journal of chemical physics*, 152(18):184102, 2020.
- [21] Kerstin Andersson, Per Åke Malmqvist, Björn O. Roos, Andrzej J. Sadlej, and Krzysztof Wolinski. Second-order perturbation theory with a CASSCF reference function. *Journal of Physical Chemistry*, 94(14):5483–5488, 1990.